

Nitrogen bonding configurations at nitrated Si(001) surfaces and Si(001)-SiO₂ interfaces: A first-principles study of core-level shifts

G.-M. Rignanese

*Unité de Physico-Chimie et de Physique des Matériaux, Université Catholique de Louvain, 1 Place Croix du Sud,
B-1348 Louvain-la-Neuve, Belgium*

Alfredo Pasquarello

*Institut Romand de Recherche Numérique en Physique des Matériaux (IRRMA), Ecole Polytechnique Fédérale de Lausanne (EPFL),
PPH-Ecublens, CH-1015 Lausanne, Switzerland*

(Received 28 July 2000; published 24 January 2001)

Using a first-principles approach, we investigate nitrogen bonding configurations at nitrated Si(001) surfaces and Si(001)-SiO₂ interfaces by comparing calculated core-level shifts with measured photoemission spectra. Fully relaxed model structures are generated in which N atoms occur in a variety of positions and bonding configurations that include, in particular, H nearest neighbors and dangling bonds. By establishing a correspondence between the bonding environment of the N atoms and their 1*s* core-level shifts, we provide a scheme for the interpretation of experimental photoemission spectra for both the nitrated surface and the nitrated interface. We also calculate Si 2*p* core-level shifts focusing on the effects of Si-N bonds, and find good agreement with experiment also in this case.

DOI: 10.1103/PhysRevB.63.075307

PACS number(s): 79.60.Jv, 68.35.-p, 73.20.-r

I. INTRODUCTION

Silicon dioxide (SiO₂) is the most extensively used dielectric in the microelectronics industry. By thermal oxidation, thin layers of SiO₂ can easily be grown on Si substrates. The resulting Si-SiO₂ interface shows a very small amount of interface states and excellent electrical properties. However, as the scale of integration increases and the thickness of the dielectric is reduced, the performance of SiO₂ is degraded due to leakage currents and to its permeability to boron and alkali-metal ion diffusion.¹ These problems have stimulated the investigation of a large variety of alternative dielectrics. Because the dielectric that will eventually replace SiO₂ has not yet been identified, nitrated silicon oxides (SiO_xN_y) or even silicon nitrides (SiN_xH_y) appear as interesting ways to meet the requirements of ultra-large-scale integration (ULSI) technology for the near future.² Nitrated silicon oxides display reduced interface state generation,³ higher dielectric breakdown values and reliability,^{4,5} improved *I-V* and *C-V* characteristics,⁶ and increased resistance to ionizing radiation.⁷ In the case of silicon nitrides, their higher dielectric constant permits the use of physically thicker films while retaining the same *C-V* performance as that of thinner oxide layers.⁸ In this context, the thermal nitridation by ammonia (NH₃) has attracted considerable attention. Indeed, the NH₃ can either be adsorbed at the Si(001)-2×1 surface⁹ to produce ultrathin, sharp Si(001)-SiN_xH_y interfaces, or used to incorporate N at the Si(001)-SiO₂ interface.¹⁰ In the latter case, also other oxidation agents have been employed, such as nitrous oxide N₂O (Refs. 3,10, and 11) or nitric oxide NO.^{6,12}

Because the insulating layer required for ULSI devices may be only tens of angstroms thick, the knowledge of the detailed atomic structure of the interface is becoming critical for further improving the performance of electronic devices.

Among the various experimental techniques, x-ray photoemission spectroscopy (XPS) is particularly sensitive to the various bonding configurations of nitrogen and silicon atoms by recording N 1*s* or Si 2*p* core levels. Indeed, XPS has been one of the principal experimental tools for the investigation of both nitrated Si(001) surfaces,^{13–18} and nitrated Si(001)-SiO₂ interfaces.^{3,10–12,19–26} However, the interpretation of the experimental spectra in terms of N or Si bonding configurations is not always straightforward and often leads to some controversy. For instance, as we shall see hereafter, the main peak in the N 1*s* experimental spectra for the Si(001)-SiO₂ interface has been attributed to nearest-neighbor configurations as different as N-Si₃, N-Si₂ (involving a dangling bond), N-Si₂H, or even N-Si₂O. The large variety of techniques that have been used to engineer the nitrogen concentration and composition profiles contribute to this uncertainty. Indeed, different techniques may lead to different bonding configurations and therefore to different values of the core-level shifts.

We recently showed that by complementing the XPS measurements with a theoretical approach that gives core-level shifts based on first-principles calculations, a quite satisfactory picture can be reached for the understanding of the underlying bonding configurations of the N atoms at both nitrated Si(001) surfaces²⁷ and nitrated Si(001)-SiO₂ interfaces.²⁸ However, these previous investigations have not covered all the possible N configurations that have been suggested in the literature. For instance, the presence of dangling bonds at the surface or at the interface, which has frequently been invoked in experimental work,^{3,12,20,29} has not been addressed by theory so far.

The purpose of this work is to provide a comprehensive interpretation of N 1*s* core-level shifts at nitrated Si(001) surfaces and at nitrated Si(001)-SiO₂ interfaces. We include in the present study new bonding configurations such as N

atoms carrying dangling bonds or forming N-H bonds in both systems. In order to provide a full description of the bonding properties at these nitrated surfaces and interfaces, we also calculate Si $2p$ core-level shifts induced by the formation of N-Si bonds in these systems.

Several model surfaces and interfaces containing N atoms in different bonding configurations are considered. Using a first-principles approach, the atomic positions are relaxed and the N $1s$ and Si $2p$ core-level shifts calculated. From these results we derive a comprehensive picture of the N $1s$ and Si $2p$ core-level shifts in these systems. In fact, because of the similar overall dielectric environment at Si(001) surfaces and Si-SiO₂ interfaces, core-level shifts for atoms with the same nearest neighbors in any of the two systems are generally found to be close.

This work is organized as follows. In Sec. II, we discuss the technical details of the first-principles methods used for relaxing the model surfaces and interfaces and for calculating the core-level shifts. Section III is dedicated to nitrated Si(001) surfaces. We describe structural models and discuss the N $1s$ and Si $2p$ core-level shifts. Section IV is devoted to nitrated Si(001)-SiO₂ interfaces. First, we obtain new structures with N atoms either forming N-H bonds or carrying dangling bonds. Then, we compare our calculated N $1s$ and Si $2p$ core-level shifts with experimental data. Finally, our conclusions are presented in Sec. V. We examine here the validity of a general relation between N and Si bonding configurations and XPS data holding for both the surface and the interface.

II. TECHNICAL ASPECTS

In all our calculations, the atomic positions are fully relaxed using a damped molecular-dynamics method,^{30,31} which provides the electronic structure as well as the forces that act on the ions. Only valence electrons are explicitly considered using pseudopotentials (PPs) to account for core-valence interactions. A norm-conserving PP is employed for Si atoms,^{32,33} while the H, N, and O atoms are described by ultrasoft PPs.³⁴

The N $1s$ and Si $2p$ core-level shifts are calculated including core-hole relaxation. The final-state effects are accounted for by considering total energy differences.³⁵ A detailed description is given in Ref. 36. In order to obtain good structural properties, the wave functions and the augmented electron density were expanded on plane-wave basis sets defined by cutoffs of 30 and 150 Ry, respectively. In all our calculations, the Brillouin zone (BZ) was sampled using only the Γ point. For our smallest unit cell (with a 2×2 interface unit), we found that calculated core-level shifts were affected by less than 0.1 eV when doubling the size of the cell. Because this error is within the accuracy of our approach, this justifies the use of the sole Γ point for sampling the Brillouin zone.

The use of the local-density approximation (LDA) (Ref. 37) to density-functional theory for the calculation of core-level shifts in molecules already proved successful in the case of N $1s$ (Ref. 28) and Si $2p$ (Ref. 38) levels. Overall, the agreement between experiment and theory was found to

TABLE I. Relative N $1s$ core-level shifts for a series of molecules. Experiment from Ref. 43. The shifts are given in eV and a positive sign for Δ indicates higher binding energies.

| Molecule | Δ^{LDA} | Δ^{IA} | Δ^{GGA} | Δ^{expt} |
|-----------------------------------|-----------------------|----------------------|-----------------------|------------------------|
| NH ₃ | 0.00 | 0.00 | 0.00 | 0.0 |
| NH ₂ CH ₃ | -0.57 | -0.47 | -0.49 | -0.5 |
| NH(CH ₃) ₂ | -0.58 | -0.73 | -0.64 | -0.7 |
| N(CH ₃) ₃ | -0.61 | -0.71 | -0.72 | -0.8 |
| NH ₂ COH | 1.13 | 1.03 | 1.00 | 0.8 |
| NO ₂ | 7.24 | 7.00 | 6.90 | 7.3 |
| N ₂ O(N*NO) | 3.30 | 3.08 | 3.14 | 3.1 |
| (NN*O) | 7.08 | 6.85 | 6.80 | 7.0 |
| CINO | 5.68 | 5.53 | 5.51 | 5.8 |

be very good with values differing by less than a few tenths of an eV for a broad range of shifts. More recently, we showed that, in the case of N $1s$ shifts, the use of the generalized gradient approximation (GGA) (Ref. 39) leads to a slightly better description of shifts induced by N-H bonds.²⁷ We therefore used the GGA for calculating N $1s$ shifts. For Si $2p$ shifts, we instead used the LDA to allow for a comparison with previous calculations.³⁶ Throughout this paper, pseudopotentials are always constructed consistently with the chosen functional for the exchange and correlation energy.⁴⁰

In general, we consistently relaxed the structure using the same density functional used for the calculation of the core-level shifts. However, in particular cases, we also made use of the intermediate approximation (IA), which consists in using the LDA for relaxing the atomic positions and the GGA for computing core-level shifts.^{41,42} In order to test the performance of the IA, we considered the same set of molecules that we had used in our previous studies.^{27,28} This set does not contain molecules with N-Si bonds, for which we were unable to find measured shifts in the literature. Because of the broad range of shifts, we nevertheless considered this set sufficiently representative for testing the accuracy of our approach. The calculated N $1s$ core-level shifts are summarized in Table I, where they are compared with the experimental values.⁴³ The agreement with experiment is very good within the three approaches (LDA, GGA, and IA) over the full range of considered shifts. In particular, the difference between the GGA and the IA is negligible (less than 0.1 eV) showing that the difference between the LDA and the GGA is essentially due to a better treatment of the screening of the core hole rather than to an improved description of the structural properties. In the following, we will therefore use the IA for structural models that were previously relaxed in the LDA, without proceeding to a new, computationally expensive relaxation in the GGA. For instance, we resort to the IA for the interface models obtained in Ref. 28.

III. NITRIDED SI(001) SURFACES

A. Structural models

To model nitrated Si(001) surfaces, we consider a 2×2 square surface unit with a side based on the theoretical equi-

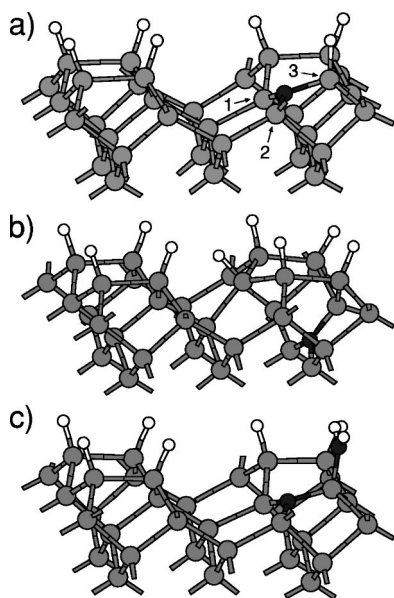


FIG. 1. Models of the NH_3 exposed $\text{Si}(001)\text{-}2\times 1$ surface with N atoms in N-Si_3 configurations: (a) reference model for N 1s (Ref. 27), (b) model with the N atom located deeper in the substrate, (c) model with a second-nearest-neighbor N atom belonging to a surface $-\text{NH}_2$ group. The N, Si, and H atoms are represented in black, gray, and white, respectively.

librium lattice constant of bulk Si. This parameter is adjusted consistently with the exchange-correlation functional used for the atomic relaxation ($a=10.82$ and 10.95 Å for LDA and GGA, respectively). The dimension of the cell in the direction orthogonal to the surface is $c=15.9$ Å, containing eight monolayers of Si (about 9 Å). The bottom extremities were saturated with hydrogen atoms.

In previous work, we studied the dependence of N 1s core-level shifts on the number of H atoms in the first nearest-neighbor shell.²⁷ In the present study, we extend this investigation to N atoms carrying a dangling bond. Since our approach only gives relative core shifts, it is important to define a reference configuration that can reliably be associated to one of the experimental peaks. As a reference, we took the model in Fig. 1(a) in which the N atom is bonded to three Si atoms (N-Si_3). In order to check the robustness of this choice, we also considered two variants as shown in Figs. 1(b) and 1(c). Both variants show N atoms in N-Si_3 configurations. However, in the model in Fig. 1(b) the N atom is deeper in the substrate, while in the model in Fig. 1(c) the N atom in a N-Si_3 configuration presents a N atom in its second-nearest-neighbor shell. The configurations in Figs. 1(b) and 1(c) can therefore be used to examine the sensitivity of our reference to enhanced screening conditions and to further neighbors, respectively.

Model surfaces with N atoms carrying a dangling bond were generated using as a starting configuration the model shown in Fig. 2(a).²⁷ A twofold-coordinated N atom was obtained by removing the H atom from the first-nearest-neighbor shell of the N atom. This gives a HSi-N-SiH bridge structure that can also be obtained by inserting a N atom in one of the Si dimers of the H-saturated $\text{Si}(001)2\times 1$ surface

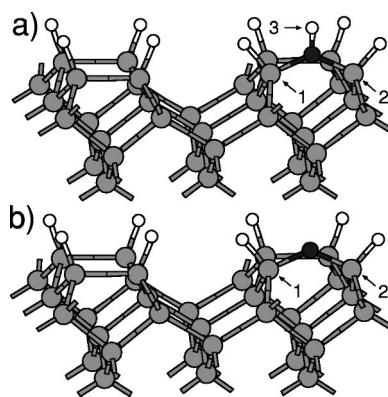


FIG. 2. Models of the NH_3 exposed $\text{Si}(001)\text{-}2\times 1$ surface with N atoms (a) forming N-H bonds ($\text{N-Si}_2\text{H}$) (Ref. 27) and (b) carrying a dangling bond (N-Si_2).

[see Fig. 2(b)]. Three different charge states of the dangling bond were considered: positive ($\text{N}^+\text{-Si}_2$), neutral ($\text{N}^0\text{-Si}_2$), and negative ($\text{N}^-\text{-Si}_2$).

Finally, we also investigated the dependence of the N 1s shifts on the coverage. All the models discussed so far correspond to a partial coverage of $1/4$ of a NH_3 molecule per Si dimer. As a test case, we considered the model in Fig. 3(a), which corresponds to the generally accepted picture for the NH_3 adsorption on the $\text{Si}(001)$ surface.⁴⁴ In order to avoid steric effects, we attached the NH_2 groups on opposite sides of adjacent Si-Si dimers in a chess-board pattern. The NH_2 groups adopt the same local geometry as in the case of partial coverage.

For all these models, the positions of the atoms were fully relaxed with the exception of the atoms belonging to the three lowest Si monolayers of the substrate, which were kept fixed in their crystalline positions. In general, the structural properties of our models compare very well with previous theoretical studies.⁴⁵⁻⁴⁹ For the model structure in Fig. 3(a), the agreement between calculated and measured structural

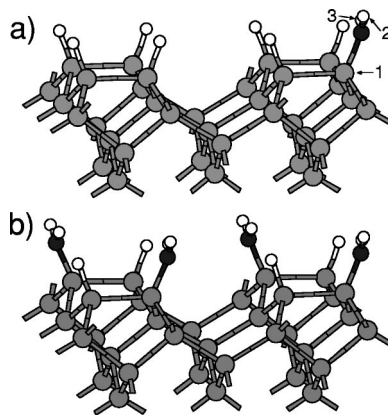


FIG. 3. Models of the NH_3 exposed $\text{Si}(001)\text{-}2\times 1$ surface with N atoms in N-SiH_2 configurations: (a) partial coverage of $1/4$ NH_3 per Si dimer (Ref. 27) and (b) full coverage of one NH_3 molecule per Si dimer. The four NH_2 groups are attached on opposite sides of adjacent Si dimers in a chess-board pattern in order to minimize steric effects.

TABLE II. Structural properties for the model of the nitrated surface shown in Fig. 3(a), as obtained within the LDA and the GGA. For the bond angles, we adopt the notation of Ref. 48. We distinguish the parameters referring to HSi-SiNH₂ dimers from those related to HSi-SiH dimers by labeling the former ones with an asterisk. The experimental values are taken from Ref. 44.

| Bond lengths (Å) | LDA | GGA | Expt. |
|---------------------------|------|------|------------|
| N-Si | 1.69 | 1.76 | 1.73 |
| N-H | 1.03 | 1.03 | |
| Si-Si* | 2.40 | 2.47 | |
| Si-Si | 2.38 | 2.44 | |
| Si-H | 1.50 | 1.52 | |
| Bond angles (°) | LDA | GGA | Expt. |
| $\theta_{\text{Si-Si}}^*$ | -1 | 0 | 8 ± 8 |
| $\theta_{\text{Si-Si}}$ | 0 | 0 | |
| $\phi_{\text{Si-N}}$ | 25 | 28 | 21 ± 4 |
| $\phi_{\text{Si-H}}^*$ | 20 | 22 | |
| $\phi_{\text{Si-H}}$ | 20 | 22 | |
| ψ | 163 | 153 | |
| H-N-H | 112 | 111 | |

parameters is also very good,⁴⁴ as can be seen from Table II. For the other structures, an experimental characterization is not available. We therefore only give the bond lengths between the N atom and its first nearest neighbors (Table III).

As a by-product of the structural relaxation, we found that the HSi-NH-SiH bridge model shown in Fig. 2(a) is more stable than the HSi-SiNH₂ model in Fig. 3(a) by 0.57 eV, 0.22 eV, and 0.25 eV within the LDA, the IA, and the GGA, respectively. This observation suggests a similarity with the H₂O-exposed Si(001)-2×1 surface. Indeed, it was found that the HSi-O-SiH configuration is more stable than the HSi-SiOH by 0.3 eV.⁵⁰ However, it is generally accepted that, at room temperature, the water molecule adsorbs dissociatively to form HSi-SiOH,^{51–53} and that the O atom inserts into the Si dimer only upon annealing.^{54,55}

B. N 1s core-level shifts

The N 1s photoemission spectrum shows an important peak at approximately the same energy as in bulk Si₃N₄,^{13–15,17,18} and another one shifted at $\Delta = 2.7$ eV higher

TABLE III. Bond lengths, calculated within the GGA, between the N atom and its first nearest neighbors (X_n , where n refers to the labels in Figs. 1–3), as found in the nitrated Si(001) surface models. The bond lengths are given in Å.

| Model | Fig. | X_1 | X_2 | X_3 | $d(\text{N}-X_1)$ | $d(\text{N}-X_2)$ | $d(\text{N}-X_3)$ |
|---------------------------------|------|-------|-------|-------|-------------------|-------------------|-------------------|
| N-Si ₃ | 1(a) | Si | Si | Si | 1.84 | 1.84 | 1.87 |
| N-Si ₂ H | 2(a) | Si | Si | H | 1.78 | 1.78 | 1.03 |
| N ⁺ -Si ₂ | 2(b) | Si | Si | | 1.68 | 1.68 | |
| N ⁰ -Si ₂ | 2(b) | Si | Si | | 1.68 | 1.68 | |
| N ⁻ -Si ₂ | 2(b) | Si | Si | | 1.69 | 1.69 | |
| N-SiH ₂ | 3(a) | Si | H | H | 1.76 | 1.03 | 1.03 |

TABLE IV. Relative N 1s shifts at nitrated Si(001) surfaces: comparison between experiment and theory. Measured shifts and their tentative assignments are compared to calculated shifts and their corresponding configurations. The N-Si₃ configuration is taken as the reference. The shifts are given in eV.

| Δ^{expt} | Assignment | Ref. | Δ^{theor} | Configuration |
|------------------------|---------------------|-------------|-------------------------|---------------------|
| 0.0 | N-Si ₃ | 13–15,17,18 | 0.00 | N-Si ₃ |
| 0.6–0.7 | N-Si ₂ H | 15 | 0.66 | N-Si ₂ H |
| | N-SiH ₂ | 18 | | |
| 1.1–1.2 | N-Si ₂ H | 13 | 1.09 | N-SiH ₂ |
| | N-SiH ₂ | 14,15,17 | | |

binding energy.^{13–15,18} These two peaks are generally attributed to a N atom bonded to three Si atoms (N-Si₃), and to the formation of a condensed NH₃ layer physisorbed at the surface, respectively. While a general consensus has been reached for these two assignments, the interpretation of the intermediate peaks observed at $\Delta = 0.6\text{--}0.7$ eV (Refs. 15 and 18) and $\Delta = 1.1\text{--}1.2$ eV (Refs. 13–15 and 17) has been quite controversial, as can be seen from Table IV.

In order to compare shifts of different structural models, it is necessary to align the core-level shift scales. This was achieved by aligning the bulk Si 2*p* core-level shift, which is common to all the models. The bulk Si 2*p* level was obtained by an average over the shifts of atoms located in the sixth and seventh layer of the substrate (counting from the interface).

We associate the reference core-level shift of the model in Fig. 1(a) to the principal experimental peak that occurs at approximately the same position as in bulk Si₃N₄. This reference is found to be robust with respect to the variations considered in Figs. 1(b) and 1(c), which gave core-level shifts as small as $\Delta = -0.03$ eV and $\Delta = -0.13$ eV, respectively.

In our previous study,²⁷ we found N 1s shifts of $\Delta = 0.66$ and 1.09 eV for the N-Si₂H model [Fig. 2(a)] and the N-SiH₂ model [Fig. 3(a)], respectively, as reported in Table IV. These results are in excellent agreement with the experimental data and support the interpretation that assigns a shift of about 0.6 eV per N-H bond.¹⁵ In this work, we further examine these assignments by investigating models that include a dangling bond [Fig. 2(b)]. We found $\Delta = -1.84$ eV, -1.79 eV, and -1.75 eV for the N⁺-Si₂, the N⁰-Si₂, and the N⁻-Si₂ configurations, respectively. Thus, the shift Δ associated to the presence of a dangling bond on the N atom is about -1.8 eV, independent of the charge state. This value does not correspond to any of the experimental peaks and suggests that twofold-coordinated N atoms do not occur in significant amounts upon nitridation of the Si(001) surface by NH₃.

For the model with a full coverage of the surface [Fig. 3(b)], we found the same core-level shifts as for the partial coverage in Fig. 3(a). This result further demonstrates that core-level shifts are barely affected as long as the immediate vicinity of the excited atom remains unchanged.

TABLE V. Relative Si $2p$ shifts at nitrated Si(001) surfaces: comparison between calculated and measured values. The Si bulk line is taken as the reference.

| Configuration | Δ^{theor} (eV) | Δ^{exp} (eV) | Ref. |
|-----------------------------------|------------------------------|----------------------------|-------|
| Si-Si ₄ | 0.00 | 0.0 | |
| Si-Si ₃ H | 0.16–0.26 | 0.3 | 16,18 |
| Si-Si ₃ N | 0.61–0.86 | 0.5–0.7 | 16–18 |
| Si-Si ₂ NH | 0.90–0.95 | | |
| Si-Si ₂ N ₂ | 1.28 | 1.5 | |
| Si-N ₄ | | 2.4 | |

C. Si $2p$ core-level shifts

The Si $2p$ experimental spectra of the nitrated Si surface generally show two surface peaks besides the Si substrate peak. One of these peaks is shifted by 0.3 eV to higher binding energies with respect to the bulk peak^{16,18} and is assigned to a Si atom bonded to a H atom (Si-Si₃H configuration) by comparison with other adsorbates that also give rise to Si-H bonding at the surface. The other peak is located at $\Delta = 0.5\text{--}0.7$ eV (Refs. 16–18) and is attributed to a Si atom bonded to NH₂ groups (Si-Si₃N configuration) or, equivalently, to a Si⁺¹ nitridation state. When the nitridation process is long enough to lead to the growth of a Si₃N₄ layer, higher nitridation states can also be observed. In particular, peaks were observed at $\Delta = 1.5$ eV (Refs. 16–18) and $\Delta = 2.5$ eV,^{17,18} and were assigned to the nitridation states Si⁺² (Si-Si₂N₂) and Si⁺⁴ (Si-N₄), respectively. In our different models, Si atoms with various bonding configurations occur so that we can calculate Si $2p$ core-level shifts for various nitridation states. The agreement with experimental data is very good, as can be seen from the comparison in Table V.

IV. NITRIDED Si(001)-SiO₂ INTERFACES

A. Structural models

We consider here structural models of the Si(001)-SiO₂ interface, which include nitrogen atoms forming N-H bonds or carrying dangling bonds. Together with our previous investigation in which we considered threefold-coordinated N atoms forming bonds with Si and O atoms,²⁸ this study now covers all the most likely configurations of N atoms at nitrated Si-SiO₂ interfaces.

For the model generation, we adopt as a starting point one of the Si(001)-SiO₂ interface models used in Ref. 36. In this model, a crystalline form of SiO₂, tridymite, is attached to Si(001). The model shows an abrupt transition between the oxide and the Si substrate. The bond density mismatch at the interface is accommodated by the formation of silicon dimers. Therefore, this structure does not present unsaturated dangling bonds, in accord with the extremely low density of defect states measured at this interface. The model structure used here consists of a periodically repeated orthorhombic cell containing a 2×2 square interface unit. The side of the square unit $a = 7.74$ Å (7.65 Å) is based on the theoretical equilibrium lattice constant of bulk Si within the GGA

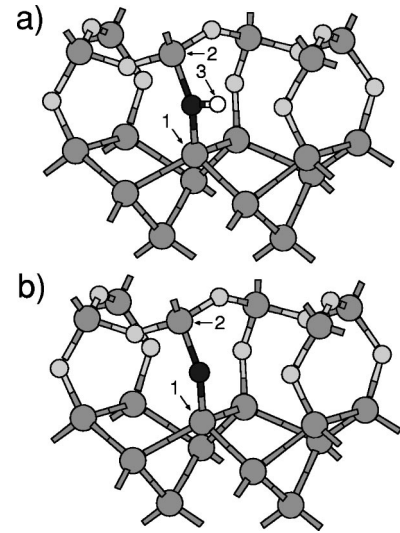


FIG. 4. Models of the nitrated Si(001)-SiO₂ interface where the N atoms replace O atoms in the neighborhood of the interface (Ref. 36): (a) the dangling bond of the N atom is saturated by a H atom leading to a N-Si₂H bonding configuration, (b) the N atom remains twofold coordinated and carries a dangling bond. The N, Si, O, and H atoms are represented in black, gray, light gray, and white, respectively.

(LDA). The dimension of the cell in the direction orthogonal to the interface is $c = 19.1$ Å, containing five monolayers of SiO₂ (~ 6.5 Å) and six monolayers of Si (~ 7.5 Å). The extremities are saturated with H atoms.

Although the long-range disordered nature of the oxide is not described within this model, this limitation does not affect the calculated values of the core-level shifts because the overall dielectric environment is well reproduced. This is confirmed by the small variations of calculated Si $2p$ shifts found for models in which the tridymite oxide was replaced with a β -cristobalite form of SiO₂.³⁶

The nitrated interface structures are obtained by incorporating in various ways a single N atom in this interface model. In order to generate configurations with N atoms forming N-H bonds or carrying dangling bonds, we proceeded as follows. We replaced one of the O atoms in the neighborhood of the interface by a N atom. Then, the remaining unsaturated bond on the N atom is either satisfied by a H atom [Fig. 4(a)] or left dangling [Fig. 4(b)]. In the former case, the N atom is in a N-Si₂H configuration. In the latter case, we have a N⁺-Si₂, N⁰-Si₂, or N⁻-Si₂ configuration, according to the charge state of the dangling bond. By the same procedure, we also generated another model with a N-Si₂H configuration, in which the nitrogen atom is introduced deeper in the oxide, as shown in Fig. 5.

After the incorporation of the N atoms, all the oxide atoms as well as the first three Si layers were fully relaxed. In Table VI, we report the bond lengths of the incorporated N atom with its first nearest neighbors. These results are within 1% of the experimental values for molecules with similar nitrogen-bonding configurations,⁵⁶ suggesting that our relaxed models give a good representation of the local structure for the various bonding configurations. This is further

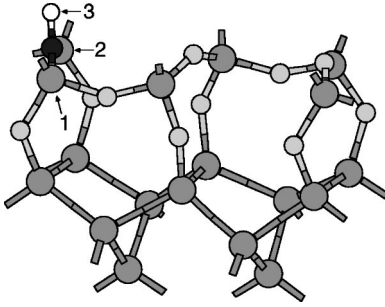


FIG. 5. Model of the nitrided Si(001)-SiO₂ interface where the N atom replaces an O atom located deeper in the oxide (Ref. 36). The dangling bond of the N atom is saturated by a H atom leading to a N-Si₂H bonding configuration.

confirmed by a more detailed analysis of the structural properties, which can be found elsewhere.⁵⁷ It is interesting to note that while in our previous study²⁸ it was necessary to use an $\sqrt{8} \times \sqrt{8}$ interface unit to fully relax the local structure around the incorporated N atom, the 2×2 unit proved sufficient in the present work. This is related to the way the N atoms are introduced at the interface. When a N atom replaces an O atom, as done in the present work, it can be accommodated very easily because it remains twofold coordinated to the remainder of the structure and because the Si-N bond length (~ 1.7 Å) is close to the Si-O one (~ 1.6 Å). However, when a N atom is introduced substitutionally to a Si atom, as in Ref. 28, the overall relaxation of the network is more important, not only because the N atom then forms three bonds with the network, but also because of the sizable difference between N-Si (~ 1.7 Å) and Si-Si (2.35 Å) bond lengths. Note also that the 2×2 interface unit is sufficiently large for the calculated core-level shifts not to be affected by more than 0.1 eV by the use of a neutralizing background or by the interaction with periodic images.³⁶

B. N 1s core-level shifts

The experimental spectra show a broad principal peak, approximately at the same energy as in bulk Si₃N₄, which could in principle be assigned to N atoms bonded to three Si atoms (N-Si₃). However, the unexpectedly large spread observed in the N-Si₃ binding energy has given rise to conflicting interpretations.^{3,11,12,20} Some research groups^{3,20} inter-

TABLE VI. Bond lengths, calculated within the GGA, between the N atom and its first nearest neighbors (X_n , where n refers to the labels in Figs. 4 and 5), as found in the nitrided Si(001)-SiO₂ interface models. The bond lengths are given in Å.

| Model | Fig. | X_1 | X_2 | X_3 | $d(N-X_1)$ | $d(N-X_2)$ | $d(N-X_3)$ |
|---------------------------------|------|-------|-------|-------|------------|------------|------------|
| N-Si ₃ | | Si | Si | Si | 1.81 | 1.82 | 1.81 |
| N-Si ₂ H | 4(a) | Si | Si | H | 1.71 | 1.77 | 1.04 |
| N ⁺ -Si ₂ | 4(b) | Si | Si | | 1.70 | 1.64 | |
| N ⁰ -Si ₂ | 4(b) | Si | Si | - | 1.68 | 1.66 | |
| N ⁻ -Si ₂ | 4(b) | Si | Si | - | 1.66 | 1.68 | |
| N-Si ₂ H | 5 | Si | Si | H | 1.71 | 1.76 | 1.04 |

preted this large linewidth as evidence for the presence of N-Si₂ (i.e., a twofold-coordinated N atom carrying a dangling bond) or N-Si₂H configurations. Bouvet *et al.*²² suggested that the dispersion resulted from N atoms in N-Si₃ configurations but with a differing number of O atoms in their next-nearest-neighbor shell. The latter explanation was fully supported by our previous calculations,²⁸ and later received additional support from another theoretical investigation.⁵⁸ In more recent experimental work, a careful examination of the correlation between the N-Si₃ peak position and the areal density of nitrogen also corroborated this picture.²⁵ Another experimental study, in which the N profile was modified by reoxidation, also reached the same conclusion.⁵⁹

The presence of other, well separated, XPS peaks has also been debated. Indeed, due to the large variety of sample preparation techniques, the data in the literature differ significantly from one experimental work to another. Some XPS spectra show no evidence for any other peak in a range of ± 3 eV from the N-Si₃ peak.^{11,19} In other experiments, a second distinct peak is observed at $\Delta = 1.6$ – 3.0 eV (Refs. 10,12,21,22, and 24–26) and attributed to N-Si₂O configurations. Shallenberger *et al.*²⁵ observed a third peak at $\Delta = 5.3$ eV that they attributed to N-SiO₂ configurations. More recently, Chang *et al.*²⁶ found a third and even a fourth peak at $\Delta = 3.8$ and 6.1 eV and assigned them in terms of N-SiO₂ and N-O₃ configurations, respectively. Hence, the identification of N bonding configurations involving oxygen atoms remains quite uncertain.

In order to address this complex set of experimental data, we extend in the present study the N bonding configurations under consideration to cover H atoms and dangling bonds. The scope is twofold. First, we intend to verify whether our initial interpretation for the principal peak still holds in the presence of new evidence concerning other bonding configurations. Second, we hope to be able to shed new light on the interpretation of the other peaks in the spectra by covering an extended set of bonding configurations. Since we decided to present N 1s core-level shifts consistently within the GGA, we recalculated within the IA the core-level shifts for the configurations with N-O bonds obtained previously within the LDA.²⁸

The core shifts obtained for the different structural models in our calculations were aligned using the bulk Si 2p line. This was obtained by averaging over Si atoms located in the fourth and fifth layer of the substrate. We chose as a reference the shift of the N-Si₃ configuration in which the N atom is located most deeply in the Si substrate, i.e., the same as in Ref. 28. The calculated N 1s shifts for the various interface models are reported in Table VII. For the N-Si₂H configurations, the calculated shift ($\Delta = 0.4$ eV) occurs within the linewidth of the principal experimental peak. Therefore, we conclude that both N-Si₃ and N-Si₂H could contribute to this peak. However, for N-Si₂ configurations, the calculated shift $\Delta \approx -1.9$ eV falls out of the range of the main peak. Hence, these results definitely rule out the possibility that both N-Si₃ and N-Si₂ configurations contribute to the main peak, as suggested in Ref. 3.

TABLE VII. Relative N $1s$ shifts for the nitrated Si(001)-SiO₂ interface models. The nitrogen atoms differ either by their location or by their bonding configuration. The shifts are given with respect to the N-Si₃ configuration in which the N atom is located most deeply in the Si substrate. The location of the N atom is given in terms of the distance z from the plane determined by the lowest suboxide Si atoms.

| Configuration | $z(\text{\AA})$ | Δ^{theor} (eV) |
|---------------------------------|-----------------|------------------------------|
| N-Si ₃ | -0.8 | 0.00 |
| | -0.7 | 0.10 |
| | 3.4 | 0.47 |
| N ⁺ -Si ₂ | 1.5 | -1.92 |
| N ⁰ -Si ₂ | 1.5 | -1.99 |
| N ⁻ -Si ₂ | 1.5 | -1.88 |
| N-Si ₂ H | 1.5 | 0.39 |
| | 4.1 | 0.45 |
| N-Si ₂ O | -0.6 | 1.60 |
| | 3.6 | 1.92 |
| N-SiO ₂ | 3.7 | 3.81 |

In light of the results in Table VII, the interpretation of the other experimental peaks remains difficult. The second peak at $\Delta = 1.6\text{--}3.0$ eV (Refs. 10,12,21,22,24, and 25) can reasonably be attributed to N-Si₂O configurations, for which we found a shift of $\Delta = 1.60\text{--}1.92$ eV. However, it appears difficult to associate the third peak, observed by Shallenberger *et al.* at $\Delta = 5.3$ eV and attributed to a N-SiO₂ configuration,²⁵ to our value of 3.81 eV calculated for such a configuration in the neighborhood of the interface. However, as we showed in Ref. 28, the core-level shifts depend on the distance from the interface and Δ can increase by as much as 0.8 eV at a distance of about of 50 \AA . Thus, because the oxide layer in Ref. 25 is thicker than 50 \AA , the interpretation adopted by Shallenberger *et al.* cannot definitely be ruled out.

It is particularly interesting to compare our calculated shifts with the experimental work of Chang *et al.*,²⁶ because of the large number of peaks in their XPS spectra. Our inability to determine shifts on an absolute scale allows two competitive schemes for interpreting the experimental peaks. The peak identified as N-1 could be assigned to N-Si₃ configurations, while the peaks labeled N-2, N-3, and N-4 would then correspond to N-Si_{3-x}O_x configurations with $x = 1, 2$, and 3, respectively. Alternatively, one could assign the N-2 peak to N-Si₃. The peaks N-3 and N-4 would correspond to configurations with an increasing number of O atoms in the first neighbor shell (N-Si₂O and N-SiO₂), while the remaining N-1 peak could be attributed to N-Si₂ dangling-bond configurations. These two interpretation schemes are compared in Table VIII.

The agreement with our calculated shifts is quite good in both cases. However, given the accuracy of the calculations, factors other than the binding energies should be considered for reaching a definite assignment. In a recent experimental work, it was found that the N $1s$ binding energy associated to N-Si₃ configurations at the interface is larger by 0.4 eV

TABLE VIII. Alternative interpretation schemes for the binding energies (BEs) measured by Chang *et al.*²⁶ at nitrated Si(001)-SiO₂ interfaces. In the first scheme, the N-Si₃ configuration is assigned to the N-1 peak, while in the second scheme the N-Si₃ configuration is assigned to the N-2 peak (the dangling bond N-Si₂ configuration being assigned to the N-1 peak). The shifts are given in eV.

| First scheme | BE | Δ^{expt} | Δ^{theor} | Configuration |
|---------------|-------|------------------------|-------------------------|----------------------|
| N-1 | 397.5 | 0.0 | 0.00 | N-Si ₃ |
| N-2 | 399.2 | 1.8 | 1.60-1.92 | N-Si ₂ O |
| N-3 | 401.3 | 3.8 | 3.81 | N-SiO ₂ |
| N-4 | 403.6 | 6.1 | 5.55 | N-O ₃ (?) |
| Second scheme | BE | Δ^{expt} | Δ^{theor} | Configuration |
| N-1 | 397.5 | -1.8 | -1.75 | N-Si ₂ |
| N-2 | 399.2 | 0.0 | 0.00 | N-Si ₃ |
| N-3 | 401.3 | 2.0 | 1.60-1.92 | N-Si ₂ O |
| N-4 | 403.6 | 4.3 | 3.81 | N-SiO ₂ |

^aThis result was obtained for the molecule (H₃SiO)₃N using the LDA.²⁸

with respect to the N $1s$ binding energy in bulk Si₃N₄.⁵⁹ This measurement favors the second interpretation scheme, because in the experiment by Chang *et al.* the N-2 peak was also found at higher binding energies than in Si₃N₄ (by 0.6 eV), whereas the N-1 peak occurred at 1.2 eV *lower* binding energies. The second interpretation scheme is also supported by the relative intensities of the N-1 and N-2 peak. In fact, N-2 is found to be significantly more intense than N-1. According to the second interpretation scheme, this would imply that the amount of regularly bonded N-Si₃ configurations is much larger than that of N-Si₂ dangling-bond configurations, which appears plausible. While assuming the first interpretation scheme, we would conclude that N-Si₂O is more likely to occur than N-Si₃, in contrast to the structure of crystalline Si₂N₂O.⁶⁰ The most intriguing aspect of adopting the second interpretation scheme is the occurrence of N dangling bonds. The large number of N $1s$ peaks in the spectra measured by Chang *et al.* and their behavior upon annealing suggests that highly energetic structures might occur in their samples and that the occurrence of N dangling bonds can thus not be ruled out *a priori*. However, important support in favor of the second interpretation scheme would come from a distinct experimental observation pointing to the presence of N dangling bonds.

C. Si $2p$ core-level shifts

X-ray photoemission spectroscopy on Si $2p$ core levels has been used extensively for studying Si(001)-SiO₂ interfaces both prior to⁶¹⁻⁶³ and after^{10,11,19,23} nitridation. In the absence of nitrogen, the XPS spectrum generally shows two principal lines, corresponding to SiO₂ and Si. The SiO₂ line, which is shifted by $\Delta = 3.8$ eV to higher binding energies with respect to the Si bulk line, results from Si atoms that are fourfold coordinated by O atoms. The XPS spectra also show three intermediate oxidation states of silicon that are charac-

TABLE IX. Relative Si $2p$ shifts Δ for selected Si atoms in the nitrated Si(001)-SiO₂ interface models, compared to experimental values. The selected silicon atoms differ either by their location or by their bonding configuration. The location of Si atoms is given in terms of the distance z from the plane determined by the lowest suboxide Si atoms. The shifts are given with respect to a Si atom located deep in the substrate, representative of the Si bulk line.

| Configuration | z (Å) | Δ^{theor} (eV) | Δ^{expt} (eV) | Ref. |
|----------------------|---------|------------------------------|-----------------------------|-------|
| Si-Si ₄ | -3.8 | 0.00 | 0.0 | |
| Si-Si ₃ O | 0.0 | 1.19-1.24 | 1.0 | 11,63 |
| Si-Si ₃ N | -2.2 | 1.06 | 0.7 | 16,18 |
| | 1.1 | 0.92 | | |

teristic of the transition region and are generally assigned to Si atoms with an increasing number of O atoms in their first neighbor shell.⁶¹⁻⁶³ This interpretation of the intermediate oxidation states has lately given rise to some controversy,⁶⁴ but has received strong confirmation by first-principles calculations.^{36,65} Very recently, the apparent inconsistencies at the origin of the controversy were satisfactorily explained.^{66,67}

We focus here on the effect of Si-N bonding on Si $2p$ shifts and refer to Ref. 36 for a complete discussion on Si-O bonding at Si-SiO₂ interfaces. We selected Si atoms in the interface models with one N and three Si nearest neighbors (Si-Si₃N). For comparison, we also considered Si atoms bonded to one O and three Si atoms (Si-Si₃O). Calculated Si $2p$ core-level shifts are given in Table IX, where the location of the considered Si atoms is also specified. For Si atoms in Si-Si₃O configurations, we calculated shifts of about 1.2 eV, which compare well with the experimental value of 1.0 eV.^{11,63} This result fully agrees with previous calculations that showed a systematic overestimation by about 20%.^{36,68}

For Si atoms in Si-Si₃N configurations, we found shifts of about 1 eV, which should be compared with the measured shift of 0.7 eV.^{16,17} Despite the overestimation, theory and experiment show the same trends, namely both give smaller Si $2p$ shifts for Si-N than for Si-O bonds. This is in agreement with the simple picture deriving from the electronegativity difference between O and N atoms. Replacing an O by a N atom increases the electronic charge density on the Si atom and gives a shift of the Si $2p$ peak towards lower binding energies. However, this simple picture only considers the initial state, whereas the calculation shows that initial and final state effects are often of the same order.³⁶ The small difference between N- and O-induced chemical shifts (about 0.2 eV) might explain the difficulties that experimentalists experience in highlighting the N contribution in Si $2p$ XPS spectra of oxynitrides.¹¹

V. CONCLUSIONS

In this work, we have presented a comprehensive study of N $1s$ and Si $2p$ photoemission data at NH₃-exposed Si(001)

TABLE X. Comparison between calculated core-level shifts at the nitrated Si(001)-2 \times 1 surface and at the nitrated Si(001)-SiO₂ interface. The shifts are defined with respect to references described in the text.

| Configuration | Core level | Δ (eV) | |
|----------------------|------------|---------------|-----------|
| | | Surface | Interface |
| N-Si ₂ H | N $1s$ | 0.4 | 0.6 |
| N-Si ₂ | N $1s$ | -1.8 | -1.9 |
| Si-Si ₃ N | Si $2p$ | 0.9 | 0.9-1.1 |

surfaces and nitrated Si(001)-SiO₂ interfaces. Several model surfaces and interfaces containing N and Si atoms in different bonding configurations have been investigated. Using a first-principles approach, the atomic structures were fully relaxed and the corresponding N $1s$ and Si $2p$ core-level shifts were calculated. Based on these calculations, we established a correspondence between the bonding environment of the N atoms and their N $1s$ core-level shifts measured in photoemission experiments. Calculated Si $2p$ core-level shifts affected by the formation of Si-N bonds were also found to agree well with the available experimental data.

In the case of NH₃ adsorbed Si(001) surfaces, our study provides a clear interpretation scheme for the bonding configurations of the N atoms. According to this scheme, the peaks in the XPS spectra associated to chemisorbed N species can all be interpreted in terms of threefold-coordinated N atoms with a varying number of Si and H nearest neighbors, i.e., N-Si_{1-x}H_x with $x=0, \dots, 2$. Every additional H atom in the nearest-neighbor shell produces a contribution to the N $1s$ core-level shift of about 0.6 eV to higher binding energies.^{15,27} The XPS spectra do not show a peak at the predicted location for N atoms carrying dangling bonds ($\Delta = -1.8$ eV). We therefore conclude that these defect configurations do not occur during nitridation of the Si(001) surface by NH₃.

At nitrated Si(001)-SiO₂ interfaces, our investigation also provides a clear picture for interpreting XPS spectra. The principal peak results from N atoms threefold coordinated by Si atoms, the large linewidth and the asymmetry being caused by second-nearest-neighbor effects.^{22,28,58,59} The contribution to the principal peak from N atoms with one H and two Si nearest neighbors cannot be ruled out ($\Delta = 0.4$ eV) and will depend on the concentration of incorporated H atoms. The formation of N-O bonds gives rise to additional peaks at higher binding energies, and their precise location in the spectrum depends on the profile of the N concentration. In fact, the shifts depend by as much as 0.8 eV on the overall dielectric environment determined by the distance of the N atoms to the Si substrate.²⁸ According to our calculations, it also appears clearly that nitrogen atoms carrying dangling bonds do not contribute to the principal peak, as previously suggested in the literature.³ Instead, such configurations might be at the origin of a peak observed in highly defective samples, at lower binding energies with respect to the main peak ($\Delta = -1.9$ eV).²⁶

In conclusion, it should be noted that the overall dielectric

environments at the nitrided Si(001) surface and the nitrided Si(001)-SiO₂ interface are not too different [$\epsilon_{\infty}=2.1$ for SiO₂ (Ref. 69) with respect to $\epsilon_{\infty}=1$ for vacuum]. This explains why the N 1s core-level shifts in both systems can be interpreted in terms of a common scheme that primarily depends on the atoms in the nearest-neighbor shell. In fact, N and Si atoms with the same-nearest neighbor configuration in the two systems are found to give approximately the same shifts, as can be seen in Table X.

ACKNOWLEDGMENTS

We acknowledge useful discussions with J. P. Chang and J. Eng. Jr. G. -M. R. was supported by the Belgian Program on Interuniversity Attraction Poles initiated by the Belgian Federal Office for Scientific, Technical and Cultural Affairs. A. P. acknowledges support from the Swiss National Science Foundation under Grants Nos. 21-52'182.97 and 620-57850.99. The calculations were performed on the NEC-SX4 of the Swiss Center for Scientific Computing (CSCS).

- ¹L.C. Feldman, E.P. Gusev, and E. Garfunkel, in *Fundamental Aspects of Ultrathin Dielectrics on Si-based Devices*, edited by E. Garfunkel, E. Gusev, and A. Vul (Kluwer, Dordrecht, 1998), pp. 1–24.
- ²M.L. Green *et al.*, Appl. Phys. Lett. **65**, 848 (1994).
- ³E.C. Carr and R.A. Buhrman, Appl. Phys. Lett. **63**, 54 (1993).
- ⁴M.Y. Hao, W.M. Chen, K. Lai, and C. Lee, Appl. Phys. Lett. **66**, 1126 (1995).
- ⁵S.B. Kang, S.O. Kim, J.-S. Byun, and H.J. Kim, Appl. Phys. Lett. **65**, 2448 (1994).
- ⁶Z.-Q. Yao, H.B. Harrison, S. Dimitrijevic, D. Sweatman, and Y. T. Yeow, Appl. Phys. Lett. **64**, 3584 (1994).
- ⁷S.T. Chang, N.M. Johnson, and S.A. Lyon, Appl. Phys. Lett. **44**, 316 (1984).
- ⁸Y. Ma and G. Lukovsky, J. Vac. Sci. Technol. B **12**, 2504 (1994).
- ⁹A. Izumi and H. Matsumura, Appl. Phys. Lett. **71**, 1371 (1997).
- ¹⁰M. Bhat *et al.*, Appl. Phys. Lett. **64**, 1168 (1994).
- ¹¹Z.H. Lu, S.P. Tay, R. Cao, and P. Pianetta, Appl. Phys. Lett. **67**, 2836 (1995).
- ¹²R.I. Hegde *et al.*, Appl. Phys. Lett. **66**, 2882 (1995).
- ¹³F. Bozso and P. Avouris, Phys. Rev. Lett. **57**, 1185 (1986).
- ¹⁴E.K. Hlil, L. Kubler, J.L. Bischoff, and D. Bolmont, Phys. Rev. B **35**, 5913 (1987).
- ¹⁵J.L. Bischoff, F. Lutz, D. Bolmont, and L. Kubler, Surf. Sci. **251/252**, 170 (1991).
- ¹⁶C.U.S. Larsson, C.B.M. Andersson, N.P. Prince, and A.S. Flodström, Surf. Sci. **271**, 349 (1992).
- ¹⁷C.H.F. Peden, J.W. Rogers, N.D. Shinn, K.B. Kidd, and K.L. Tsang, Phys. Rev. B **47**, 15 622 (1993).
- ¹⁸G. Dufour, F. Rochet, H. Roulet, and F. Sirotti, Surf. Sci. **304**, 33 (1994).
- ¹⁹D.G.J. Sutherland *et al.*, J. Appl. Phys. **78**, 6761 (1995).
- ²⁰S.R. Kaluri and D.W. Hess, Appl. Phys. Lett. **69**, 1053 (1996).
- ²¹H.C. Lu *et al.*, Appl. Phys. Lett. **69**, 2713 (1996).
- ²²D. Bouvet *et al.*, J. Appl. Phys. **79**, 7114 (1996).
- ²³A. Kamath *et al.*, Appl. Phys. Lett. **70**, 63 (1997).
- ²⁴B.C. Smith and H.H. Lamb, J. Appl. Phys. **83**, 7635 (1998).
- ²⁵J.R. Shallenberger, D.A. Cole, and S.W. Novak, J. Vac. Sci. Technol. A **17**, 1086 (1999).
- ²⁶J.P. Chang *et al.*, J. Appl. Phys. **87**, 4449 (2000).
- ²⁷G.-M. Rignanese and A. Pasquarello, Appl. Phys. Lett. **76**, 553 (2000).
- ²⁸G.-M. Rignanese, A. Pasquarello, J.-C. Charlier, X. Gonze, and R. Car, Phys. Rev. Lett. **79**, 5174 (1997).
- ²⁹H. Ono *et al.*, Appl. Phys. Lett. **74**, 203 (1999).
- ³⁰R. Car and M. Parrinello, Phys. Rev. Lett. **55**, 2471 (1985).
- ³¹A. Pasquarello, K. Laasonen, R. Car, C. Lee, and D. Vanderbilt, Phys. Rev. Lett. **69**, 1982 (1992); K. Laasonen, A. Pasquarello, R. Car, C. Lee, and D. Vanderbilt, Phys. Rev. B **47**, 10 142 (1993).
- ³²G.B. Bachelet, D.R. Hamman, and M. Schlüter, Phys. Rev. B **26**, 4199 (1982).
- ³³A. Dal Corso, A. Pasquarello, A. Baldereschi, and R. Car, Phys. Rev. B **53**, 1180 (1996).
- ³⁴D. Vanderbilt, Phys. Rev. B **41**, 7892 (1990).
- ³⁵E. Pehlke and M. Scheffler, Phys. Rev. Lett. **71**, 2338 (1993).
- ³⁶A. Pasquarello, M.S. Hybertsen, and R. Car, Phys. Rev. Lett. **74**, 1024 (1995); Phys. Rev. B **53**, 10 942 (1996).
- ³⁷J.P. Perdew and A. Zunger, Phys. Rev. B **23**, 5048 (1981).
- ³⁸A. Pasquarello, M.S. Hybertsen, and R. Car, Phys. Scr. **T66**, 118 (1996).
- ³⁹J.P. Perdew, J.A. Chevary, S.H. Vosko, K.A. Jackson, M.R. Pederson, D.J. Singh, and C. Fiolhais, Phys. Rev. B **46**, 6671 (1992).
- ⁴⁰M. Fuchs, M. Bockstedte, E. Pehlke, and M. Scheffler, Phys. Rev. B **57**, 2134 (1998).
- ⁴¹L. Fan and T. Ziegler, J. Chem. Phys. **94**, 6057 (1991).
- ⁴²C. Massobrio, A. Pasquarello, and A. Dal Corso, J. Chem. Phys. **109**, 6626 (1998).
- ⁴³W.L. Jolly, K.D. Bomben, and C.J. Eyermann, At. Data Nucl. Data Tables **31**, 433 (1984).
- ⁴⁴N. Franco *et al.*, Phys. Rev. Lett. **79**, 673 (1997).
- ⁴⁵R.-H. Zhou, P.-L. Cao, and S.-B. Fu, Surf. Sci. **249**, 129 (1991).
- ⁴⁶N.W. Moriarty and P.V. Smith, Surf. Sci. **265**, 168 (1992).
- ⁴⁷E. Fattal, M. Radeke, G. Reynold, and E. Carter, J. Phys. Chem. B **101**, 8658 (1997).
- ⁴⁸S.-H. Lee and M.-H. Kang, Phys. Rev. B **58**, 4903 (1998).
- ⁴⁹R. Miotto, G.P. Srivastava, and A.C. Ferraz, Phys. Rev. B **58**, 7944 (1998).
- ⁵⁰B.B. Stefanov and K. Raghavachari, Surf. Sci. **289**, L1159 (1997).
- ⁵¹Y.J. Chabal, Phys. Rev. B **29**, 3677 (1984).
- ⁵²P.A. Thiel and T.E. Madey, Surf. Sci. Rep. **7**, 211 (1987).
- ⁵³A. Vittadini, A. Selloni, and M. Casarin, Phys. Rev. B **52**, 5885 (1995).
- ⁵⁴M.K. Weldon, B.B. Stefanov, K. Raghavachari, and Y.J. Chabal, Phys. Rev. Lett. **79**, 2851 (1997).
- ⁵⁵B.B. Stefanov and K. Raghavachari, Appl. Phys. Lett. **73**, 824 (1998).
- ⁵⁶*Landolt-Börnstein: Numerical Data and Functional Relationships in Science and Technology*, edited by O. Madelung (Springer-Verlag, Berlin, 1982), Vol. II/7.

- ⁵⁷G.-M. Rignanesi, Ph.D. thesis, Université Catholique de Louvain, 1998. A postscript file is available at the following URL: <http://www.pcpm.ucl.ac.be/~rigna/docs/thesis.ps.gz>
- ⁵⁸G.F. Cerofolini, A.P. Caricato, L. Meda, N. Re, and A. Sgamelotti, *Phys. Rev. B* **61**, 14 157 (2000).
- ⁵⁹Y. Miura, H. Ono, and K. Ando, *Appl. Phys. Lett.* **77**, 220 (2000).
- ⁶⁰J. Anthony, R. Bideaux, K. Bladh, and M. Nichols, *Handbook of Mineralogy, Vol. 3, Halides, Hydroxides, Oxides* (Mineral Data Publishing, Tucson, AZ, 1997).
- ⁶¹P.J. Grunthaner, M.H. Hecht, F.J. Grunthaner, and N.M. Johnson, *J. Appl. Phys.* **61**, 629 (1987).
- ⁶²F.J. Himpsel, F.R. McFeely, A. Taleb-Ibrahimi, and J.A. Yarmoff, *Phys. Rev. B* **38**, 6084 (1988).
- ⁶³Z.H. Lu, M.J. Graham, D.T. Jiang, and K.H. Tan, *Appl. Phys. Lett.* **63**, 2941 (1993).
- ⁶⁴M.M. Banaszak Holl, and F.R. McFeely, *Phys. Rev. Lett.* **71**, 2441 (1993).
- ⁶⁵A. Pasquarello, M.S. Hybertsen, and R. Car, *Phys. Rev. B* **54**, R2339 (1996).
- ⁶⁶K. Raghavachari and J. Eng, Jr., *Phys. Rev. Lett.* **84**, 935 (2000).
- ⁶⁷K. Raghavachari, A. Pasquarello, J. Eng, Jr., and M.S. Hybertsen, *Appl. Phys. Lett.* **76**, 3873 (2000).
- ⁶⁸A. Pasquarello, M.S. Hybertsen, G.-M. Rignanesi, and R. Car, in *Fundamental Aspects of Ultrathin Dielectrics on Si-based Devices* (Ref. 1), pp. 89–102.
- ⁶⁹H.R. Philipp, in *Handbook for Optical Constants of Solids*, edited by E.D. Palik (Academic, San Diego, 1998), p. 749.